NUMERICAL ACCURACY WHEN SOLVING THE FEL EQUATIONS*

R.R. Lindberg †, ANL Advanced Photon Source, Argonne, IL 60439, USA

Abstract

The usual method of numerically solving the FEL equations involves dividing both the e-beam and radiation field into "slices" that are loaded one at a time into memory. This scheme is only first order accurate in the discretization of the ponderomotive phase because having only one slice in memory effectively results in a first order interpolation of the field-particle coupling. While experience has shown that FEL simulations work quite well, the first order accuracy opens the door to two possible ways of speeding up simulation time. First, one can consider higher order algorithms; unfortunately, these methods appear to require all the particle and field data in memory at the same time, and therefore will typically only be important for either small (probably 1D) problems or for parallel simulations run on many processors. Second, one may consistently solve the equations to some low order using faster, simpler algorithms (replacing, for example, the usual RK4). The latter is particularly attractive, although in practice it may be desirable to retain higher order methods when integrating along z. We investigate some of the possibilities.

INTRODUCTION

Numerical simulation of free-electron lasers (FELs) is an integral part of understanding existing FEL devices and planning for future machines. Presently there are several codes (Ginger [1], genesis 1.3 [2], FAST [3], MEDUSA [4], etc.) that have shown remarkable agreement with experimental measurements. While the current FEL algorithms are based on several physical approximations designed to increase their speed and efficiency, certain problems can still require many hours (or even weeks/months) of CPU time. Here we discuss some of the factors that play a role in FEL simulation time, and show an algorithm that can reduce the computational time for certain FEL problems by a factor of two without sacrificing numerical stability or accuracy.

For simplicity, the present paper predominantly restricts itself to treating the FEL equations in 1D, but our general discussion is relevant to the full 3D system. We begin by reviewing some of the numerical algorithms/tricks used to reduce computational time, and show that for time dependent simulations the resulting FEL codes are limited to being first order accurate in the discretization of the ponderomotive phase. Hence, traditional FEL codes at best converge $\sim(\Delta\theta)$. Before more fully discussing time dependence, however, we introduce some of the issues regarding numerical accuracy using the single frequency/time independent equations. We present an explicit algorithm that integrates the FEL interaction while exactly conserving the total (kinetic + field) energy, and compare its performance to more the traditional second and fourth order Runge-Kutta solvers, abbreviated by RK2 and RK4, respectively.

Then, we turn to the fully time dependent equations. Here, we show how to develop a fully second order (in both Δz and $\Delta\theta$) FEL algorithm. However, this method requires that all the particles and field data be simultaneously accessible in memory, and hence is probably only practical for small problems or those run on multiple processors. Furthermore, the accuracy requirements for a typical FEL simulation do not require a fully second order method, and we show that our conservative algorithm is probably sufficient for almost all problems, and is twice as fast as the typical RK4 scheme. Finally, we indicate how our conservative 1D algorithm can be extended to 3D.

NUMERICALLY SOLVING THE 1D FEL EQUATIONS

The longitudinal FEL particle phase space is comprised of the ponderomotive phase $\theta_j \equiv (k_u + k_1)z - ck_1t_j$ and the scaled energy difference (Lorentz factor) $\eta_j \equiv (\gamma_j - \gamma_r)/\gamma_r$. Here, the coordinate z is the distance along the undulator and t_j is the particle time, while $k_u \equiv 2\pi/\lambda_u$ and $k_1 \equiv 2\pi/\lambda_1$ are the undulator and resonant radiation wavevector, respectively, which are related to the reference energy γ_r through the FEL resonance condition $\lambda_1 = \lambda_u(1 + K^2/2)/2\gamma_r^2$ (the undulator deflection parameter $K \equiv eB_0/mck_u$, with B_0 being the peak magnetic field and e, m, c the electron charge magnitude, mass, and the speed of light).

We use the standard Bonifacio-Pelligrini-Narducci scaling for high gain FELs [5], defining the scaled energy, distance, and electric field via $\hat{\eta} \equiv \eta/\rho$, $\hat{z} \equiv 2\rho k_u z$, and $a(\theta,\hat{z}) \equiv [eK[\mathrm{JJ}]/(\rho^2 mc^2\gamma_r^2)]E(\theta;\hat{z})$; the dimensionless FEL parameter ρ is given by

$$\rho \equiv \left[\frac{1}{8\pi}\frac{I}{I_A}\left(\frac{K^2[\mathrm{JJ}]}{1+K^2/2}\right)^2\frac{\gamma_r\lambda_1^2}{2\pi\sigma_x^2}\right]^{1/3}, \qquad (1)$$

where I is the peak current, $I_A \equiv 4\pi\epsilon_0 mc^3/e \approx 17$ kA is the Alfvén current, ϵ_0 is the permittivity of free space, σ_x is the rms beam size, and the Bessel function factor $[\mathrm{JJ}] \equiv J_0[K^2/(4+2K^2)] - J_1[K^2/(4+2K^2)]$. We assume

* Work supported by U.S. Dept. of Energy Office of Basic Energy Sciences under Contract No. DE-AC02-06CH11357

† lindberg@aps.anl.gov

ISBN 978-3-95450-126-7

that the FEL equations are averaged in the phase θ over the ponderomotive length $2\pi M_{\rm ave}$, in which case the 1D FEL equations are

$$\frac{d\theta_j}{d\hat{z}} = \frac{1}{2\rho}\left[1 - \frac{1}{(1+\rho\hat{\eta}_j)^2}\right] \tag{2}$$

$$\frac{d\hat{\eta}_j}{d\hat{z}} = \frac{1}{2\pi M_{\rm ave}}\int d\theta\ \left[a(\theta,\hat{z})e^{i\theta_j} + c.c.\right] \times \frac{1}{1+\rho\hat{\eta}_j}\Pi\left(\tfrac{\theta-\theta_j}{2\pi M_{\rm ave}}\right) \tag{3}$$

$$\frac{\partial a}{\partial \hat{z}} + \frac{1}{2\rho}\frac{\partial a}{\partial \theta} = -\frac{1}{N_\lambda}\sum_{j=1}^{N_e}\frac{e^{-i\theta_j(z)}}{1+\rho\hat{\eta}_j}\Pi\left(\tfrac{\theta-\theta_j}{2\pi M_{\rm ave}}\right). \tag{4}$$

Here, N_λ is the number of (macro)particles in the $2\pi M_{\rm ave}$ wavelegnths associated with the averaging, while $\Pi(x)$ is the rectangle function that is defined to be unity if $|x| \le 1/2$ and zero otherwise. The small-efficiency ($\Delta\gamma_j/\gamma_0 = \rho\hat{\eta}_j \ll 1$) limit obtains by setting $\rho \to 0$ above.

Traditional FEL algorithms are based on the so-called "slice" formulation, wherein the field and electron beam are divided into a number of discrete FEL slices associated with the averaged ponderomotive length. Since the radiation from any electron only travels forward a total distance $N_u\lambda_1$, one can begin by loading into memory a single ponderomotive slice of particles from the tail of the electron beam, and record the generated field as a function of z. After discarding the particles, the field history is then used as an input when integrating the equations of motion for the next slice of particles closer to the beam head, and again the radiation produced is stored. This process repeats sequentially from tail to head until the entire output field is created. This standard FEL algorithm has very modest memory requirements, since only a small fraction of the total number of particles need be in memory at a time.

On the other hand, the algorithm's rate of convergence is no better than linear with the discretization size $\Delta\theta$. This is because evaluating the force in (3) requires knowing the field over the entire averaging length $2\pi M_{\rm ave}$. The standard FEL algorithm effectively assumes that the field is constant within each (averaged) FEL slice, so that the accuracy at best scales linearly with $\Delta\theta$. There is in principle no way to construct a fully second order scheme without abandoning the usual sequentially loaded slice formulation just described, since all the neighboring (in θ) field values are not known at the same location along $\hat{z}$.

Nevertheless, the slice formulation has been quite successful for FEL simulation largely because of the relatively short integration distances (up to saturation the errors have only accumulated over 10-15 scaled units of $\hat{z}$), the relative unimportance of the precise field profile, and because the level of energy conservation can be much better than that implied above. Specifically, the first order convergence need only apply to the precise field profile and particle trajectories. For example, the popular discrete slippage scheme, in which the field is advected forward one grid spacing $\Delta\theta$ after a determined number of steps in $\hat{z}$, exactly conserves energy and is properly causal for all values of $\Delta\theta$, so that using this method of field advection/slippage means that the degree of energy conservation is entirely determined by the numerical integration scheme applied to the FEL interation.

Nearly all of the convergence complications arise from the way in which the field and e-beam are longitudinally discretized, particularly in the evaluation of the FEL interaction for a θ-dependent electric field a. Hence, these issues only appear when there are multiple particle buckets/radiation frequencies: a periodic, single frequency system simplifies the field-particle interaction such that the FEL is governed by a coupled set of ODEs. For this reason, we will first discuss numerically integrating the FEL equations when field amplitude doesn't depend on θ (i.e., single frequency/bucket simulations), and return to the time dependent case later.

Numerical Accuracy

Comparing different FEL numerical schemes is complicated by the fact that SASE is initialized by the particle bunching due to the initially random longitudinal positions (shot noise), which makes it difficult to begin with the same initial conditions while varying the integration step size and/or the number of macroparticles. To load the same initial conditions, our particle loading scheme was designed to match the numerical bunching to that of a particular beam containing the actual number of electrons. We being with a random distribution of the actual number of electrons within a fixed number of wavelengths that is sorted by phase from smallest to largest. Starting with the electron of smallest θ, we then compute the bunching due to the number of electrons each macroparticle is designed to represent, and assign the first macroparticle's phase coordinate such that its phase gives the appropriate bunching. Hence, if the actual beam has N_e electrons that we represent with $N_{\rm macro}$ particles, we choose

$$\theta_j \ \text{ such that } \ e^{-i\theta_j} = \frac{N_{\rm macro}}{N_e}\sum_{\ell=1}^{N_e/N_{\rm macro}} e^{-i\theta_\ell}. \tag{5}$$

We repeat this process for the next collection of particles until all the macroparticle phases have been assigned.

We can then verify that a given integrator converges as $(\Delta z)^q$ (i.e., that it is a $q^{\rm th}$ order method) by numerically integrating the equations using three different step sizes $\Delta\hat{z}$, $\Delta\hat{z}/2$, and $\Delta\hat{z}/4$. From simple error analysis, the order of the method can be numerically estimated using the real and imaginary parts:

$$\frac{\Re\left[a(\Delta\hat{z}) - a(\Delta\hat{z}/2)\right]}{\Re\left[a(\Delta\hat{z}/2) - a(\Delta\hat{z}/4)\right]} \approx 2^q \tag{6}$$

$$\frac{\Im\left[a(\Delta\hat{z}) - a(\Delta\hat{z}/2)\right]}{\Im\left[a(\Delta\hat{z}/2) - a(\Delta\hat{z}/4)\right]} \approx 2^q. \tag{7}$$

The error equations (6)-(7) can be used to show that a particular implementation faithfully solves the FEL equations if $q > 0$, with larger q indicating smaller errors per

ISBN 978-3-95450-126-7

step. On the other hand, the convergence is complicated by the fact that FELs are typically simulated using a number of macroparticles that is much smaller than the actual number of electrons. If the macroparticles are loaded properly (like the loading of Eq. (5) or those of Refs [6] and [7]) the results will be almost independent of the number of macroparticles. Finally, the averaging employed to arrive at (2)-(4) introduces its own possible inconsistencies and abiguities.

Nevertheless, for most FEL simulation one is interested in answering a more pedestrian question than order of convergence: how big can we make $\Delta\hat{z}$ and $\Delta\theta$ and still faithfully reproduce the dynamics? Numerical errors less than a few percent are largely irrelevant, since uncertainties in initial conditions are typically at least that big, while variations in the output power due to the length of the ponderomotive average, the number of simulation macroparticles, and the random load of the shot noise are all on the percent level. Hence, a numerical solution is probably "good enough" if it has qualitatively the same behavior and is quantitatively accurate to less than a percent.

An Energy Conserving Numerical Scheme

The accuracy and convergence of energy conservation depends on the properties of the numerical integrator applied to the FEL interaction. For example, over macroscopic distances energy conservation decreases with $(\Delta z)^2$ for a generic second order method, while the error for the popular fourth order Runge-Kutta RK4 is $O[(\Delta z)^4]$. On the other hand, the Störmer-Verlet-type integrator

$$\theta_j^{h+1/2} = \theta_j^h + \frac{\Delta\hat{z}}{2}\frac{1}{2\rho}\left[1 - \frac{1}{(1+\rho\hat{\eta}_j^h)^2}\right] \tag{8}$$

$$a^{h+1} = a^h - \Delta\hat{z}\frac{1}{N_\lambda}\sum_{j=1}^{N_\lambda}\frac{1}{1+\rho\hat{\eta}_j^h}e^{-i\theta_j^{h+1/2}} \tag{9}$$

$$\eta_j^{h+1} = \eta_j^h + \frac{\Delta\hat{z}}{2}\left[\frac{a^h + a^{h+1}}{1+\rho\hat{\eta}_j^h}e^{i\theta_j^{h+1/2}} + c.c.\right] \tag{10}$$

$$\theta_j^{h+1} = \theta_j^{h+1/2} + \frac{\Delta\hat{z}}{2}\frac{1}{2\rho}\left[1 - \frac{1}{(1+\rho\hat{\eta}_j^{h+1})^2}\right] \tag{11}$$

is explicit and exactly conserves total energy (to machine precision). In particular, it is straightforward to show that the discrete evolution (8)-(11) implies that

$$\left|a^{h+1}\right|^2 + \frac{1}{N_\lambda}\sum_j \hat{\eta}_j^{h+1} = \left|a^h\right|^2 + \frac{1}{N_\lambda}\sum_j \hat{\eta}_j^h. \tag{12}$$

Note that in the low efficiency ($\rho = 0$) limit, the algorithm above is second order and symplectic, being the Störmer Verlet integration of an associated Hamiltonian (see [8] and references therein). The full update (8)-(11) has a local error that scales as the maximum of $(\Delta\hat{z})^3$ and $\rho\hat{\eta}_j(\Delta\hat{z})^2$. For typical x-ray FEL simulations that do not employ post-saturation taper, $\rho \ll \Delta\hat{z}$ and this algorithm is effectively second order with a global error that decreases quadratically with $\Delta\hat{z}$.

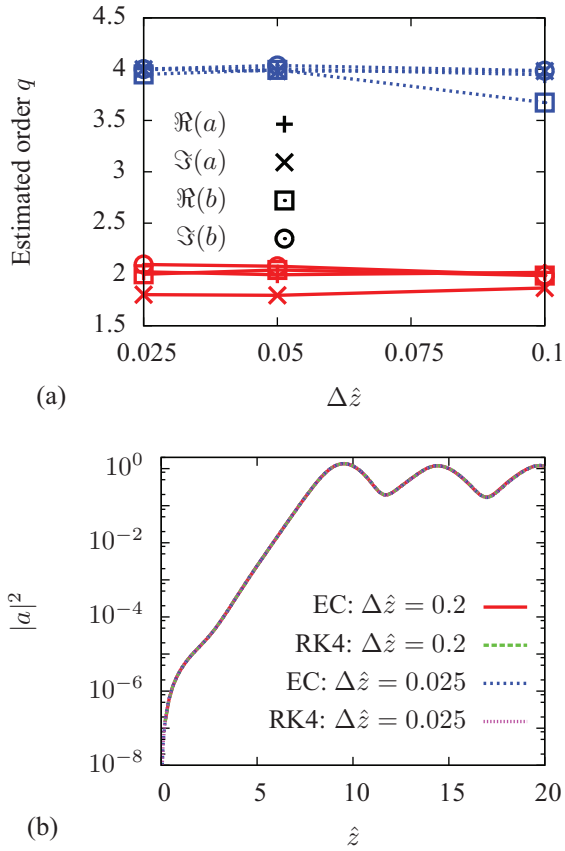

Figure 1: Comparison of the estimated convergence for the conservative scheme (red solid lines) and a standard RK4 method (blue dotted lines). Here $\Delta\hat{z}$ is the largest step size used in the formula (6)-(7) (i.e., the points at $\Delta\hat{z} = 0.1$ are derived using simulations with $\Delta\hat{z} = 0.1, 0.05$, and 0.025), and we have used both the field a and the bunching b to determine q. The conservative scheme appears to be a second order scheme since $\rho = 5 \times 10^{-4} \ll \Delta\hat{z}$. The predicted output power for two step sizes is shown in (b), where we see that for these parameters $\Delta\hat{z} = 0.2$ is sufficient.

Figure 1(a) contains results demonstrating the effectively second order nature of our energy conserving (EC) algorithm. Here, we compare numerically extracted algorithmic order q for the EC update with the standard RK4 integration scheme for various step sizes as determined by Eqs. (6) and (7) (and their analogs for the bunching b). The quoted q is the average over many final points $\hat{z}$. Since these steps sizes are larger than $\rho = 5 \times 10^{-4}$, EC converges like a second order code. Furthermore, the field profiles are nearly indistiguishable as shown in Fig. 1(b), while the EC code has approximately 2.5 times fewer operations per time step and therefore takes less than half the time to run.

Since the global error in the EC update scales as the

ISBN 978-3-95450-126-7

larger of $(\Delta\hat{z})^2$ and $\rho\hat{\eta}_j(\Delta\hat{z})$, we might worry that it would perform poorly when $\hat{\eta}_j$ approaches $1/\rho$ (i.e. $\Delta\gamma_j \to \gamma_r$). For x-ray FELs, extracting this large amount of energy is done by varying (tapering) the undulator field strength after the exponential instability has been saturated. The undulator taper serves to effectively lower the ponderomotive potential formed by the optical field, thereby extracting additional energy from the trapped electrons. Through this process it is in principle possible to convert most of the e-beam kinetic energy into field energy, so that at the end $\rho\hat{\eta}_j$ can approach unity and the EC code becomes a first order algorithm.

We have found that the EC integrator performs very well even for extreme undulator tapers that result in large changes in energy, a nice feature that we believe can be attributed to the fact that it exactly conserves energy regardless of the step size. We show this in Fig. 2, where we plot the power as a function of $\hat{z}$ for an extreme post-saturation undulator taper. In Fig. 2 we compare the results from our energy conserving (EC) update to the more standard RK2 and RK4 schemes for two different step sizes. We find that EC code predicts a final power that is within 1% of the well-converged result for $\Delta\hat{z} \leq 0.1$; the RK4 update predicts a power that is more than 5% too high when $\Delta\hat{z} = 0.1$, while the agreement is comparable for $\Delta\hat{z} = 0.2$. On the other hand, the RK2 algorithm does a poor job with the steps sizes show in the Figure, and instead requires $\Delta\hat{z} = 0.0125$ to yield a similar level of accuracy. Hence, to verify the convergence of the solutions in Fig. 2 would take almost five times longer with RK4, and about four times longer with RK2.

These findings do not contradict the order of convergence of the various algorithms, but rather point out the fact that a higher order code does not necessarily mean a more accurate one for all step sizes. In particular, we have found that for parameters like those in Fig. 2, the EC code better predicts the "true" solution than does RK4 when $\Delta\hat{z} \gtrsim 0.05$, while performing better than RK2 for all tested $\Delta\hat{z} \geq 0.00625$. Hence, we see that for step sizes typically employed for FEL simulation the EC algorithm's poor asymptotic scaling is comparatively benign, and it is fact as accurate as RK4 while being significantly faster to run.

Time Dependent Simulations

Any algorithm integrating the FEL interaction can be easily incorporated into a time dependant FEL code using the slice formulation discussed previously. For example, one can employ operator splitting to divide the EC update from the field advection (slippage), with the advection being solved, for example, by passing the field ahead an amount $\Delta\theta = \Delta\hat{z}/2\rho$ every step in $\hat{z}$. As we explained previously, however, the resulting integration scheme will only be first order accurate in the phase, even if the operator split implemented is apparently second order.

We can construct a fully second order accurate method in both $\hat{z}$ and θ by subdividing the ponderomotive length

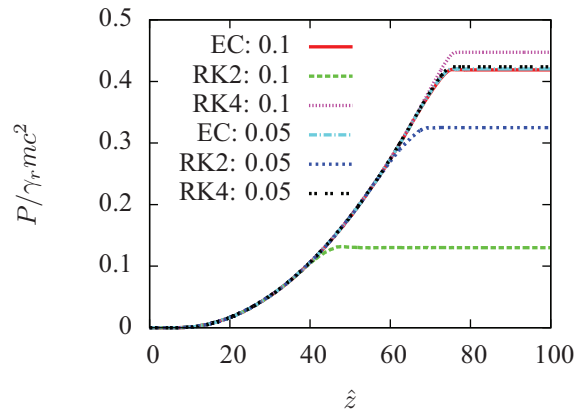

Figure 2: Comparison of the EC, RK2, and RK4 algorithms for an extreme undulator taper resulting in efficiencies approaching 50%. The EC algorithm predicts a final output power within 1% of the converged value when $\Delta\hat{z} \leq 0.1$. On the other hand, RK4 is noticably off when $\Delta\hat{z} = 0.1$, while the RK2 power agreement is very poor. For step sizes $\Delta\hat{z} \leq 0.05$ the RK4 is quite accurate, while RK2 requires even smaller step sizes, $\Delta\hat{z} \leq 0.025$.

$2\pi M_{\text{ave}}$ and linearly interpolating the field values in the energy equation (3). For example, if we use $2D$ such divisions as we show in Fig. 3 and define $x_j \equiv (\theta_{-1} - \theta_j)D/\pi M_{\text{ave}}$ so that $0 \leq x_j < 1$, then the equation of motion for the particle energy becomes

$$\frac{d\hat{\eta}_j}{d\hat{z}} = \frac{e^{i\theta_j}}{2D}\left\{ \frac{(1-x_j)^2}{2}a_{-D-1} + \left(1-\frac{x_j}{2}\right)^2 a_{-D} + \sum_{\ell=1}^{D-1}\left(a_\ell + a_{-\ell}\right) + \frac{2-(1-x_j)^2}{2}a_D + \frac{x_j^2}{2}a_{D+1}\right\} + c.c. \tag{13}$$

The source current/bunching for the field equation can be determined from (13) by invoking energy conservation. For simplicity here we only include the equation for the field a_1 assuming that there are $N_D = N_\lambda/2D$ particles per discretization $\Delta\theta$. We again split the particle phase into the part identifying the location of the field variables and the remainder x_j, so that the phase of the electron located between a_ℓ and $a_{\ell+1}$ is written as $\theta_j = \theta_{\ell,j} = \theta_\ell + x_j$ with $0 \leq x_j < 1$; note for completeness we probably should include additional subscripts on x_j identifying the θ_ℓ, but hope that its meaning is clear enough. Then, the source

ISBN 978-3-95450-126-7

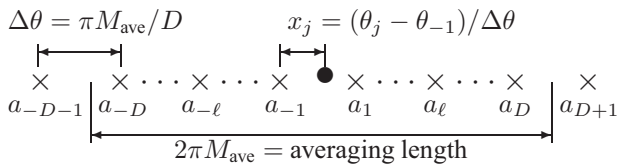

Figure 3: Diagram of the discretizations used in constructing a second order accurate algorithm to integrate the FEL interaction.

term for a_1 is

$$-\frac{1}{N_\lambda}\sum_{j=1}^{N_D}\left\{\tfrac{1}{2}x_j^2 e^{-i\theta_{-D-1,j}} + \tfrac{2-(1-x_j)^2}{2}e^{-i\theta_{-D,j}} + \sum_{\ell=-D+1}^{D-1} e^{-i\theta_{\ell,j}} + \left(1-\tfrac{x_j^2}{2}\right)e^{-i\theta_{D,j}} + \tfrac{(1-x_j)^2}{2}e^{-i\theta_{D+1,j}}\right\}. \quad (14)$$

To verify that (13), (14), and (2) is indeed second order in both z and θ, we extend the error analysis of (6)-(7) to include the dependence on $\Delta\theta$ using

$$\frac{\left\|a(\Delta\hat{z},\Delta\theta) - a(\Delta\hat{z}/2,\Delta\theta/2)\right\|}{\left\|a(\Delta\hat{z}/2,\Delta\theta/2) - a(\Delta\hat{z}/4,\Delta\theta/4)\right\|} \approx 2^q. \quad (15)$$

In (15) q now corresponds to the smallest order of the method in either $\hat{z}$ or θ, while $\|\cdot\|$ is a suitable norm that we take to separately be the vector length of the real and imaginary parts of a:

$$\|a\| \equiv \left[\sum_n (\Re\, a_n)^2\right]^{1/2} \text{ or } \left[\sum_n (\Im\, a_n)^2\right]^{1/2}. \quad (16)$$

Note that for periodic signals of fixed temporal duration q is particularly simple to compute nermically using the FFT, since in this case the frequency spacing is the same independent of $\Delta\theta$.

We show results for the numerically determined algorithmic order q in Table 1. For these results, we simulated SASE in a periodic box of 2^{14} wavelengths for a total scaled undulator length $\hat{z} = 15$, and we chose an averaging length of $M_{\rm ave} = 16$ periods. Table 1 clearly shows that the slice formulation limits the order of convergence to first order when either the EC or RK4 scheme is used to integrate the FEL interaction. On the other hand, we find that the second order method described above converges with a measured $q \geq 1.85$; our implementation here is a straightforward extension of our energy conserving (EC) algorithm.

We have shown how to develop an numerical scheme that is second order in both time (θ) and space $\hat{z}$. Extensions to higher orders are possible, but it appears unlikely that such algorithms would be useful. In particular, the second order algorithm described here is significantly more complicated to code and requires all the field and particle data to be stored in memory at the same time. Furthermore, we have shown that the formally first order energy conserving scheme EC can actually perform better than the fourth order RK4 for certain problems using typical step sizes. Hence, it seems unlikely that a fully second order (or higher) scheme is necessary at this time for FEL problems.

Table 1: Measured order of convergence q of theoretically 2nd order algorithm and the EC and RK4 integration schemes using the slice formulation. The listed $\Delta\hat{z}$ and $\Delta\theta$ are the largest used in Eq. (15).

Algorithm	$\Delta\hat{z} = 2\rho\Delta\theta = 0.1$ $\Re(a)$	$\Im(a)$	$\Delta\hat{z} = 2\rho\Delta\theta = 0.05$ $\Re(a)$	$\Im(a)$
2nd order	1.95	1.86	1.93	1.90
EC	1.07	0.59	1.03	1.28
RK4	1.08	0.60	1.02	1.30

Extensions to 3D Simulations

We have found that our energy conserving 1D FEL integration algorithm (8)-(11) has very good numerical properties, which we have attributed to the fact that it exactly conserves kinetic plus field energy for any step size. In this section we briefly show how this conservative method may be extended to the full 3D interaction.

It turns out that our EC algorithm can be easily extended to 3D if we use the angular representation of the electromagnetic field. In this case, the 3D generalizations of the particle energy equation (3) and field equation (4) are

$$\frac{d\hat{\eta}_j}{d\hat{z}} = \frac{\hat{\sigma}_x^2}{2\pi M_{\rm ave}}\int d\theta d\boldsymbol{\phi}\ \left[a e^{i(\theta_j+\boldsymbol{\phi}\cdot\boldsymbol{x}_j)} + c.c.\right] \times \frac{1}{1+\rho\hat{\eta}_j}\Pi\left(\tfrac{\theta-\theta_j}{2\pi M_{\rm ave}}\right) \quad (17)$$

$$\frac{\partial a}{\partial\hat{z}} + \frac{1}{2\rho}\frac{\partial a}{\partial\theta} + \frac{i\boldsymbol{\phi}^2}{2}a = -\frac{1}{N_\lambda}\sum_{j=1}^{N_e}\frac{e^{-i(\theta_j+\boldsymbol{\phi}\cdot\hat{\boldsymbol{x}}_j)}}{1+\rho\hat{\eta}_j}\Pi\left(\tfrac{\theta-\theta_j}{2\pi M_{\rm ave}}\right), \quad (18)$$

where $\boldsymbol{x}_j$ and $\hat{\sigma}_x$ are the electron transverse coordinate and the rms e-beam size scaled by $\sqrt{2\rho k_u}k_1$, while $\boldsymbol{\phi}$ is the transverse angle scaled by $\sqrt{k_1/2\rho k_u}$. At any angle $\boldsymbol{\phi}$ the field equation (18) is similar to its 1D counterpart with two exceptions: the additional particle phase in the FEL interaction and the oscillator-type term $\sim i(\boldsymbol{\phi}^2/2)a$ that gives diffraction. The latter can be isolated out using operator splitting (e.g., the Strang method [9]) and then solved with the energy conserving update $a(\boldsymbol{\phi},\hat{z}+\Delta\hat{z}) = a(\boldsymbol{\phi},\hat{z})e^{-i\boldsymbol{\phi}^2\Delta\hat{z}/2}$. The FEL interaction can be updated at each angle using a trivial extension to (3) that includes the additional phase; if accompanied by a similar extension to the particle energy equation (17) in which the integral over

ISBN 978-3-95450-126-7

ϕ is discretized as a sum, the full update exactly conserves

$$\sum_{n,m} \Delta\phi_x \Delta\phi_y \, |a_{n,m}|^2 + \frac{1}{N_\lambda} \sum \hat{\eta}_j \qquad (19)$$

at each step, where the field subscripts n and m label the angular coordinate in ϕ_x and ϕ_y, separately, which are discretized at a spacing of $\Delta\phi_x$ and $\Delta\phi_y$.

CONCLUSIONS

We have shown that the standard FEL slice formulation used to integrate the FEL equations is at best a first order algorithm in the discretization of the phase $\Delta\theta$. To address this issue we then introduced a scheme that is fully second order accurate; however, its increased complexity and requirement to have all particles in memory may limit its utility, particularly since the accuracy requirements for FEL simulation are relatively modest. In fact, we have presented a formally first order algorithm whose accuracy can be superior to the fourth order RK4 for large step sizes $\Delta\hat{z}$. We have argued that this is because it exactly conserves energy, and believe that this energy conserving algorithm may be of general interest since it is typically twice as fast as the RK4 update. Finally, we showed how to extend our algorithm to 3D.

REFERENCES

[1] W. M. Fawley. tech. rep. LBNL-49625 (2002).

[2] S. Reiche. Nucl. Instr. Meth. Res. A 429 (1999) 243.

[3] E.L. Saldin, E.A. Schneidmiller, and M.V. Yurkov. Nucl. Instr. Meth. Res. A 429 (1999) 233.

[4] H. P. Freund, S. G. Biedron and S. V. Milton. IEEE J. Quantum Electron. 36 (2000) 275.

[5] R. Bonifacio, C. Pellegrini, and L. M. Narducci. Opt. Commun. 50 (1984) 373.

[6] C. Penman and B.W.J. McNeil. Opt. Commun. 90 (1992) 82.

[7] W. M. Fawley. Phys. Rev. ST-AB 100 (2008) 244802.

[8] E. Hairer, C. Lubich, G. Wanner. Acta Numerica (2003) 399. http://www.math.kit.edu/ianm3/lehre/geonumint2009s/media/gni_by_stoermer-verlet.pdf

[9] G. Strang. SIAM J. Numer. Anal. 5 (1968) 506.

ISBN 978-3-95450-126-7